THE JOURNAL OF PHYSICAL CHEMISTRY B

ARTICLE

pubs.acs.org/JPCB

Atomic Force Microscopy Study of Ganglioside GM1 Concentration Effect on Lateral Phase Separation of Sphingomyelin/Dioleoylphosphatidylcholine/Cholesterol Bilayers

Ren Bao, Li Li, Feng Qiu,* and Yuliang Yang

The Key Laboratory of Molecular Engineering of Polymers, Ministry of Education, Department of Macromolecular Science, the Centre of Analysis and Measurement, Fudan University, Shanghai 200433, P. R. China

ABSTRACT: The effect of monosialoganglioside GM1 (GM1) concentration on the lateral phase separation in the sphingomyelin/1,2-dioleoyl-*sn*-glycero-3-phosphocholine/cholesterol (SM/DOPC/Chol) bilayers was studied by using atomic force microscopy. The results show that, with the increase of GM1 mol fraction (x), the dominant composition of liquid-ordered (L_o) domains changes from SM to SM/GM1 and finally to GM1. Meanwhile, the decrease of domain area (A) of the L_o phase with the increase of x follows a scaling law of $A \sim x^{-3/2}$, for $x > 0.005$, indicating that the domain growth is pinned with high GM1 concentration. Results of in situ experiments of GM1 insertion into SM/DOPC/cholesterol bilayers further supported our observations.

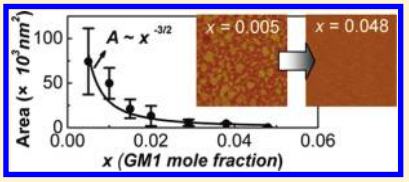

1. INTRODUCTION

Plasma membrane microdomains known as lipid rafts are rich in glycosphingolipids (GSL), sphingomyelin (SM), and cholesterol (Chol), being postulated to play a significant role in protein sorting, signal transducting, and cell growth regulating.[1−3] The formation of rafts is a result of lateral phase separation among numerous lipid species in the membranes. Generally, lipids with saturated acyl chains (e.g., GSL and SM) have higher melting temperatures (T_m) than lipids with unsaturated acyl chains (e.g., phosphatidylcholine (PC)).[1,3] When the temperature is above the T_m of lipids in membranes, lipid bilayers are in a liquid-disordered (L_d) phase, in which acyl chains are in a disordered loose-packing state. Lowering the temperature causes saturated lipids to segregate into an ordered gel phase (S_o), in which the acyl chain packing is tight. Cholesterol, another important composition of the membranes, can modulate the S_o phase into liquid-ordered (L_o) phase through filling into spaces between the acyl chains and forming hydrogen bonds with SM and GSL. In L_o phases, the acyl chain packing is tight as in S_o phases, but lipids have higher lateral mobility. The coexistence of L_o and L_d phases has been observed and studied within ternary model membranes composed of a saturated lipid, an unsaturated lipid and cholesterol, especially in the sphingomyelin/1,2-dioleoyl-*sn*-glycero-3-phosphocholine/cholesterol (SM/DOPC/Chol) systems.[4,5]

GSL molecules have shown strong influence on the phase separation in membranes due to their long saturated acyl chains and bulky oligosaccharide hydrophilic headgroups.[6,7] Unlike the well understood SM, the detailed mechanism on how the GSL affects the lateral phase separation in membranes is not clear, even for the most studied monosialoganglioside GM1. GM1 is the receptor of cholera toxin and participates in many neural activities.[8,9] Due to the repulsion between saturated and unsaturated acyl chains, GM1 can separate from unsaturated lipids, like DOPC and SOPC,[10−13] but nonaggregated GM1 molecules were also detected in DOPC-rich phase in GM1/DPPC/DOPC ternary monolayers.[14,15] On the other hand, the headgroups of GM1 induce different kinds of interactions in lipid membranes: the excluded volume effect of the bulky headgroups was used to explain the segregation between GM1 and other saturated lipids in S_o or L_o phases,[10,13,14] whereas a net of hydrogen bonds between GM1 and SM resulted in uniformly mixed phases containing GM1 and SM in GM1/SM/Chol vesicles.[16] Besides, Mao et al. pointed out the interaction between the headgroups of GM1 and the substrate could influence the phase separation in GM1/SM/Chol bilayers.[17] These complex intermolecular interactions between GM1 and saturated lipids, unsaturated lipids, and cholesterol make the lateral phase separation sensitive to the composition of the membrane. As a result, four-component mixtures composed of GM1, another saturated lipid, an unsaturated lipid, and cholesterol are needed to study the GM1 effect on membranes. In both GM1/SM/DOPC/Chol and GM1/DPPC/DOPC/Chol Langmuir−Blodgett (LB) monolayers,[14,18] GM1 molecules distribute in both L_o and L_d phases under high surface pressure. More interestingly, the size of the DPPC-rich L_o domains decreases with 0.4 mol % GM1, which could not be simply explained by the intermolecular interactions mentioned above.

Among various methods aiming to investigate lateral phase separation in membrane, atomic force microscope (AFM) is outstanding for its high resolution in detecting the changes in bilayer thickness and domain size.[19] Moreover, the planar nature of lipid bilayers makes them ideal for the detection by AFM. Thus, compared with lipid vesicles, the single supported lipid bilayers (SLBs) are suitable for AFM detection. Generally there are two methods to form SLBs on a substrate: Langmuir−Blodgett (LB) method and vesicle fusion. The latter method removes the variable of surface pressure which must be set during the

Received: January 26, 2011
Revised: April 12, 2011
Published: April 28, 2011

preparation of lipid layers by LB technique, and circumvents the issue whether there are specific interactions between the two leaflets.[20]

In this work, we investigate the GM1 concentration effect on lateral phase separation in SM/DOPC/Chol supported lipid bilayers by gradually increasing GM1 concentration in the mixture. The bilayers are formed by vesicle fusion on mica and studied in aqueous environment by AFM. Without ion addition, GM1 molecules are supposed to mainly distribute in the upper leaflet, because the mica surface is negatively charged in water and this negative surface would push the negative headgroups of GM1 molecules away from mica. We observe that increasing the GM1 mol fraction (x) in GM1/SM/DOPC/Chol mixtures leads to the component of the L_o phase changes from SM/Chol to SM/GM1/Chol, and finally to GM1/Chol. Moreover, the area of L_o domain (A) decreases with the increase of the GM1 concentration following a scaling law $A \sim x^{-3/2}$ for $x > 0.005$, which is consistent with previous computer simulation on the phase separation in a binary fluid with impurities. This decreasing trend is attributed to the pinning effect of high GM1 concentration. Further experiments of cholera toxin B-subunit (CTB) binding and in situ GM1 insertion support these observations.

2. MATERIALS AND METHODS

2.1. Materials. 1,2-Dioleoyl-*sn*-glycero-3-phosphocholine (DOPC), egg sphingomyelin (SM), and cholesterol (Chol) were purchased from Sigma-Aldrich (St. Louis, MO, USA). Methanol (CH_3OH, > 99.0%) and chloroform ($CHCl_3$, > 99.0%) were purchased from Zhenxin (Shanghai, China). Monosialoganglioside GM1 and cholera toxin B subunit were obtained from Avanti Polar Lipids Inc. (Alabaster, AL, USA). All samples were stored at −20 °C before use. Milli-Q water with a resistivity of 18.2 MΩ/cm was used in the experiment.

2.2. Preparation of Small Unilamellar Vesicles (SUVs). Chloroform/Methanol (9:1, v/v) solutions of lipids were mixed in glass vials, and were dried under a stream of nitrogen gas, then stayed in high vacuum overnight to form lipid films. The dried lipid film was resuspended with Milli-Q water to a final lipid concentration of 2.0 mg/mL. Solutions of 1.0 mg/mL were also prepared for in situ AFM experiments (Section 3.3). After hours (>4 h) incubation, giant multilamellar vesicles (GMVs) were gained in vials. The lipid suspension, consisting of GMVs was then sonicated by a tip sonicator (Xinzhi, model Scientz Jy92-II, Ningbo, Zhejiang, China) to form small unilamellar vesicles (SUVs). During the sonication, the suspensions were kept in a ice−water bath. Vesicles solutions were used immediately for bilayer preparation or stored at 4 °C for up to a week prior to use.

2.3. Bilayer Preparation. Vesicle solution (100−200 μL) was added to freshly cleaved mica clamped in a fluid cell on the AFM heater head. After incubation at 55 °C for 30 min and then being cooled to room temperature and kept for another 30 min, the bilayers were rinsed extensively with Milli-Q water to remove those excess vesicles. The occasional presence of defects allowed us to measure the bilayer thickness, confirming the presence of a single bilayer.

2.4. CTB Incubation. Before incubation with cholera toxin B subunit (CTB), the supported bilayer was well formed on mica. Then, about 100 μL of CTB water solution (1.0 μg/mL) was injected into the fluid cell. After 10 min incubation, the surface was thoroughly rinsed by Milli-Q water before further AFM imaging.

2.5. AFM Imaging. AFM images were obtained at room temperature (25 ± 1 °C) on a NanoScope IV Multimode Scanning Probe Microscope (Digital Instrument, Veeco, Santa Barbara, CA, USA) in the tapping mode using Si_3N_4 tips of V shape (model DNP-S) with spring constants of ∼0.32 N/m and resonance frequencies between 8 and 10 kHz in aqueous solutions. All experiments were conducted in Milli-Q water using a commercially available fluid cell, sealed by an O-ring. A J scanner (125 μm × 125 μm) was used with a scan rate between 0.8 and 2 Hz per line according to experimental requirements. Two or three independently prepared samples were imaged for each bilayer composition, and several different areas were scanned for each sample.

2.6. In Situ GM1 Insertion. Supported lipid bilayers composed of SM/DOPC/Chol (40:40:20, mol/mol) were prepared by SUVs solutions with the total lipid concentration at 1.0 mg/mL. This lower lipid concentration could produce more separated L_o domains, which benefited later observations. During the whole insertion experiment, the lipid bilayers were kept at 30 °C, intentionally to give more mobility to the lipids in the bilayers. A low (∼5×10^{-6} mg/mL) and a high (∼2.4×10^{-5} mg/mL) concentration of GM1 water solutions were prepared before insertion. These two concentrations both are lower than the critical micelle concentration of 5.1×10^{-3} mg/mL[21] and DLS measurement also proves no structures existing in the solutions. The GM1 water solution concentration C is calculated as follows:

$$C = \frac{5\pi(d/2)^2 Mxa_{GM1}}{VN_A(2(1-x)a_{SM} + 2(1-x)a_{DOPC} + (1-x)a_{Chol} + 100xa_{GM1})}$$

where d is the inside diameter of the fluid cell (∼5 mm), M is the molecular weight of GM1, V is the volume of the GM1 water solution injected into the fluid cell (∼0.1 mL), N_A is the Avogadro constant, x is the mole fraction of GM1 in total lipid mixtures, and a_{SM} (0.52−0.56 nm^2), a_{DOPC} (0.59−0.75 nm^2), a_{Chol} (0.08 nm^2), and a_{GM1} (0.67−1.0 nm^2) are molecular areas of SM, DOPC, cholesterol, and GM1, respectively.[22]

3. RESULTS AND DISCUSSIONS

3.1. Effect of Cholesterol on GM1 Distribution in SM/DOPC/Chol Bilayer. GSLs were observed to form ordered domains with or without the presence of cholesterol.[6] However, other experiments proved that cholesterol can modify GM1 distribution in model membranes.[23] As a first step, SM/DOPC/GM1 mixtures without cholesterol were investigated (Figure 1a), and the molar ratio of SM/DOPC was set at 1:1 with the mole fraction of GM1 x being 0.01. In Figure 1a, three kinds of regions, with different heights—0, ∼1, and ∼2 nm, respectively—are observed. In supported lipid bilayers, the top height of the liquid-disordered (L_d) phases (region with the darkest color in Figure 1) is defined to be 0 nm. Then the heights observed in the section profiles are the height differences between other phases and L_d phase. In our experiments, the unsaturated DOPC molecules form the L_d domains (with height ∼0 nm, the red line in the section profiles), while SM and GM1 form the gel-phase (S_o) domains, which are higher than the DOPC-rich L_d domains. Besides, due to the bulky headgroups, the tight-packing GM1 molecules are even higher (with height ∼1.4−2 nm) than SM molecules (with height ∼1 nm). Therefore, the highest domains in Figure 1a are GM1-rich, and the domains with the middle height are SM-rich. These GM1-rich

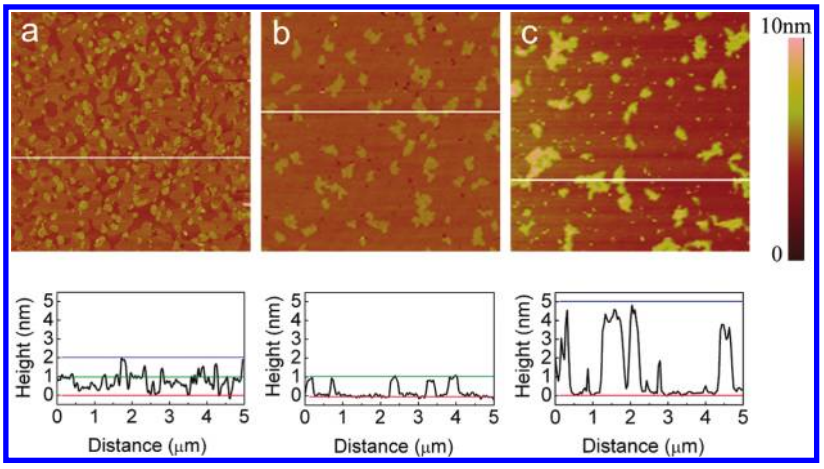

Figure 1. AFM morphologies and sections of bilayers formed from lipid vesicles. (a) the molar ratio of SM/DOPC is 1:1 with the mole fraction of GM1 x being 0.01, and (b) SM/DOPC/Chol = 2:2:1 with $x = 0.01$. After incubation with CTB water solution of 1.0 μg/mL for 10 min, the morphology of the lipid bilayer with the same composition as (b) changes, as shown in (c). The height bar is 10 nm, and the size is 5 μm × 5 μm for each image.

domains mainly stay at the edges of the SM-rich areas. A few GM1-rich domains are also found in the DOPC-rich area with height difference of ~2 nm, compared to the top of the L_d domains, which is similar to previous results in monolayers.[10,14] In addition, Figure 1a shows a small fraction of DOPC-rich phase. The possible reason may be that both SM and GM1 tend to preferentially stay in the outer leaflet, which can be observed by AFM. Indeed, the bilayer structure allows different components to spontaneously redistribute between two leaflets according to their properties and compositions.

In contrast, the phase separation between SM and GM1 are not obvious when cholesterols exist. In Figure 1b, the height differences between the higher phases and the DOPC-rich L_d phases are 1.0 ± 0.3 nm, close to the difference between SM/cholesterol and DOPC-rich phases in the literature[24] but lower than the difference between GM1-rich and DOPC-rich domains. GM1 here fails to form large GM1-rich domains as shown in Figure 1a due to the presence of cholesterol, but contributes to the fluctuation of height difference in the SM-rich liquid-ordered (L_o) phase. To further clarify the exact location of GM1 and detect the composition of the L_o domains in Figure 1b, 100 μL cholera toxin B subunit (CTB) water solution at the concentration of 1.0 μg/mL was injected into the fluid cell. After incubation for 10 min, the CTB solution was washed away by excessive water. Comparing the images before and after the incubation, we confirm that the initial bilayer was not destroyed by CTB binding at this GM1 concentration. Compared with the morphology in Figure 1b, in Figure 1c the height of the SM-rich L_o domains increased to 3.5−5.0 nm, indicating GM1 molecules mainly distribute in the previously L_o domains. Therefore, the protruding domains in Figure 1b are a mixture of GM1, SM, and cholesterol. The less high dots in the DOPC-rich domains also indicate that there are some GM1 existing in the L_d phases. Since the CTB can aggregate the GM1 molecules nearby,[25] the area of a single L_o domain in Figure 1c is larger than that in Figure 1b.

Herein, the presence of cholesterol modifies the morphology of the bilayer and no GM1-rich domains protrude from the SM-rich domains anymore in Figure 1b. GM1 and SM can act both as a hydrogen bond donor and as a hydrogen bond acceptor, whereas it is not the case for PCs.[16] However, the repulsion between chains, as well as between headgroups forces SM and GM1 to separate. Cholesterol is believed to stay within SM-rich L_o domain, acting as a hydrogen bond acceptor and a filler into the spaces under the headgroups of lipids. Therefore, a hydrogen bond net between SM and Chol molecules breaks down the van der Waals interaction between the acyl chains of SM. Similarly, a hydrogen bond net between cholesterol and GM1 can form and interrupt the GM1-GM1 interaction either. A computer simulation has proved that cholesterol is preferentially accumulating near GM1 in GM1/DPPC/cholesterol mixtures.[26] Some research even argued that with cholesterol filling between acyl chains, the repulsion between bulky headgroups of GM1 should decrease.[7] In Figure 1b, with SM, GM1 and cholesterol mixed in bilayers, a multiple hydrogen bond net between these three molecules can disperse GM1 within SM/cholesterol, resulting in an L_o phases with no obvious separation between GM1 and SM. Since GM1 molecules are dispersed in the SM-rich domains, the contribution of the headgroups of GM1 is not as strong as in Figure 1a.

3.2. Effects of GM1 Concentration. Interestingly, SM-rich domains seem to shrink in Figure 1b after the addition of GM1 into SM/DOPC/cholesterol mixtures. To understand the influence of GM1 molecules on the morphologies of SM/DOPC/cholesterol bilayers, we fixed the mole fraction of SM/DOPC/cholesterol at 2:2:1 and increased the GM1 mol fraction in total lipid mixtures. Since GM1 has been observed in both SM- and DOPC-rich domains, we set the molar ratio of GM1 against the total mole of SM/DOPC/cholesterol mixtures, not against any particular molecules. Eight mole fractions of GM1 (x) were employed: 0.001, 0.005, 0.01, 0.015, 0.02, 0.029, 0.039, and 0.048.

The morphologies of the bilayer with increasing GM1 mol fraction are shown in Figure 2. The imaging was started 45 min after the samples were cooled from the 55 °C incubation temperature. We also continuously scanned the same region of each sample to make sure no further domain growth would happen. Therefore the morphologies in Figure 2 are all in a stable state. When x is lower than 0.005 (Figure 2a,b), there are L_o domains with sizes ranging from nanometer to micrometer, the surfaces of these domains are relatively flat, and the boundaries are smooth. At $x = 0.005$, one can notice there are many small domains existing while particularly large domains disappear. The surfaces of the domains are flat but the boundaries are rough.

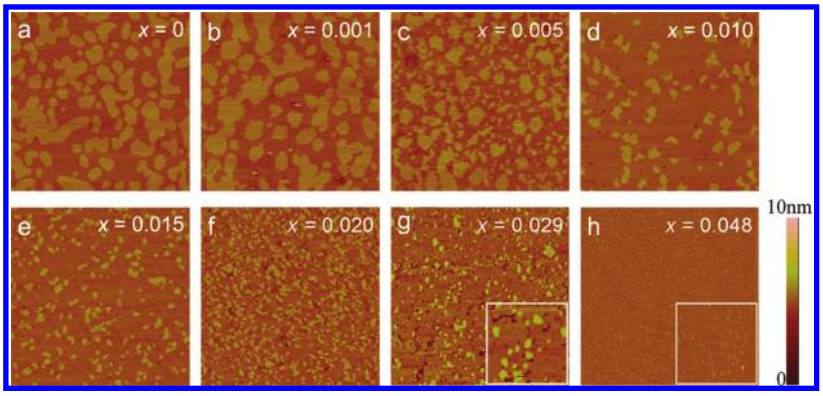

Figure 2. AFM images of SM/DOPC/cholesterol/GM1 bilayers (SM/DOPC/Chol = 2:2:1 with increasing mole fraction of GM1, x). The height bar is 10 nm and the size is 5 μm × 5 μm. The insets in Figure 2g,h are images with the size 1 μm × 1 μm.

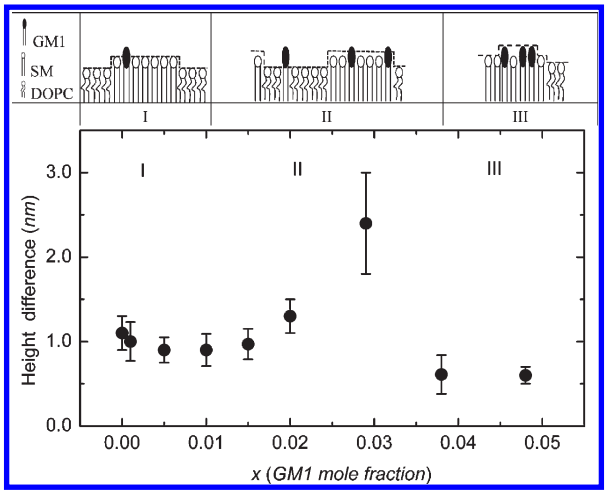

Figure 3. Statistical results of height differences between the highest domain and its surrounding phase for each composition. Illustrations (on the top) help to understand how the AFM software measures the height differences between the L_o and L_d domains: It measures the height differences between the dashed lines. For simplification, cholesterols are not included and supposed to stay in L_o phases.

When GM1 fraction x is larger than 0.01, only small domains exist and the surfaces of both the L_o and L_d phases become rougher. The domain size shrinks to several tens of nanometer when x is up to 0.048.

The average height difference between the protruding domain and its surrounding phases are obtained by employing the software Nanoscope 5.30r1. For each GM1 concentration, two or three independent examples were scanned, and the results are shown in Figure 3. The height differences can be grouped into three types according to the GM1 mol fraction (x). (I) At the low GM1 concentrations (x < 0.01): in this region the height differences are around 1.0 nm, close to the height difference between the SM/cholesterol domain and the DOPC domain in the literature[24] and in our experiment. As discussed in section 3.1, the L_o domain is composed of SM/GM1/cholesterol. CTB binding experiments were also conducted to determine the location of GM1 at lower GM1 concentrations. Figure 4 shows the morphology of the bilayers with GM1 fraction x = 0.005 after incubation with the CTB solutions for 10 min. The higher dots, which indicate the location of GM1, mainly distribute in the L_o domains at this GM1 concentration. Since the GM1 concentration is quite low, the height contributions of GM1 to the domain may be averaged by software analyses or be depressed by AFM scanning, as depicted in the upper left inset of Figure 3. (II) At the intermediate GM1 concentrations: from the point around x = 0.01, the height difference increases quickly, and is up to ~2 nm around x = 0.029, close to the typical height difference between GM1 and DOPC. The large fluctuation of height difference at x = 0.029 is due to spontaneously emerged defects during cooling process in the AFM image (Figure 2g). Therefore, it is reasonable to postulate that the L_o phases are SM/GM1-rich before x = 0.029. (III) At the high GM1 concentrations: in this region, the height differences decline to around 0.6 nm, which is the typical height difference between GM1 and SM with the presence of cholesterol as reported previously in refs 7 and 18. In the inset of Figure 2h, there are some blurry area (with relatively lower height) around the highest bright dots. Such area may contain a great amount of SM molecules, which are less higher than GM1. Therefore, AFM can only tell a smaller height difference at high GM1 concentrations (x = 0.048), as sketched in the upper right inset in Figure 3. For bilayers containing higher concentration of GM1 (x > 0.01), AFM failed to image the morphology after CTB binding, because the structure of the bilayers was destroyed by the strong CTB-GM1 binding and washing process.

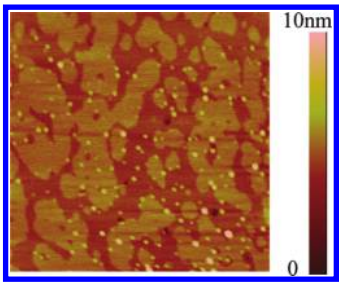

Figure 4. AFM image of SM/DOPC/Cholesterol/GM1 bilayer (SM/DOPC/Chol = 2:2:1 with x = 0.005) after incubation with CTB. The height bar is 10 nm and the size is 3 μm × 3 μm.

According to above investigations in domain height differences, the major component of the L_o phases shift gradually by adding more GM1, from SM-rich to GM1/SM mixtures, and then to GM1-rich.

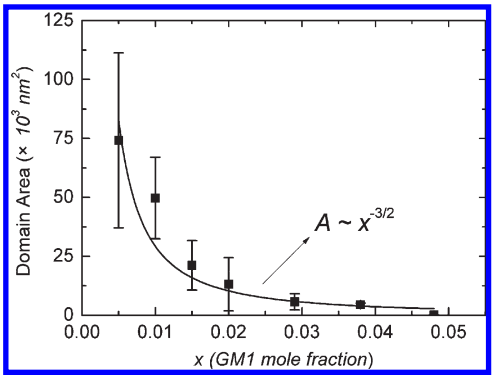

Figure 5. The dependence of the area of L_o domain (A) on the GM1 concentration (starting from $x = 0.005$). The mole ratio of SM/DOPC/Chol for each composition is 2:2:1, with the mole fraction of GM1 x in total lipid mole.

We also observed that the large SM domains (L_o) gradually degrade with the increment of GM1 concentration in the SM/DOPC/Chol/GM1 quaternary bilayers, although SM is the major component in mixtures. To quantitatively understanding the GM1 concentration influence on the domain, here domain areas of the L_o domain were measured and investigated. The statistical averaged area (A) of single L_o domains and corresponding deviation for each GM1 concentration are obtained by the software Nanoscope 5.30r1, as shown in Figure 5 (without $x = 0.001$, which was discussed later). At low GM1 concentrations, the averaged area decreases quickly; when GM1 concentration is high, A declines smoothly to several hundreds of nm^2. Along with this decrease of A, the deviation shrinks, indicating the domain sizes becoming uniform at high concentrations. This monotonically decrease in area with increasing GM1 concentration x follows a scaling law $A \sim x^{-3/2}$. This relation cannot be simply explained by hydrogen bonding or repulsion between headgroups. Besides, mainly due to its bulky headgroup, GM1 can not diffuse quickly on the surface,[7] and have a low diffusion coefficient ($\sim 10^{-9}$ cm^2/s), compared to other lipids ($\sim 10^{-8}$ cm^2/s) .[27] GM1 insertion into SM/DOPC/cholesterol bilayer also proved a ~50% decrease in fluidity.[13] Thus GM1 molecules could be recognized as fixed impurities during phase separation in the SM/DOPC/Chol membrane. Moreover, GM1 molecules show preference toward the L_o phases containing SM and cholesterol, as is discussed in section 3.1. On the other hand, the interactions between GM1 molecules and the DOPC-rich L_d phases are energetically unfavorable, as reported in refs 10 and 12. Since cholesterol is believed to stay with SM, our system can be viewed as a binary fluid ((SM + Chol)/DOPC) with fixed impurities (GM1). In this fluid, equilibrium domain size are controlled by the concentration of impurities, which has been also reported in previous computer simulation by Qiu et al.[28] They found that with the increase of the impurities concentration, the morphology of the phase separation of binary fluid changes significantly. They further proved that the saturation of fluid domain sizes (R) is determined by the competition between the interfacial energy (σ/R) between the two immiscible phases and the energy penalty due to the impurities fixed in the unfavorable phase, V_{cpl}, where σ is the interfacial tension between the two phases. The domain growth was pinned by fixed impurities favoring one phase with sufficiently high impurities density (n_0), following the scaling law $R \sim n_0^{-3/4}$, where R is the domain size, and $n_0 \propto x$ for $n_0 \simeq x/(0.8 + 0.2x) \approx x$, with $x \ll 1$ in our experiments. By a simple translation, one has domain area $A \sim R^2 \sim n_0^{-3/2} \sim x^{-3/2}$, which is in agreement with the result of our experiment.

We note that low GM1 concentration ($x = 0.001$) does not strongly affect the domain morphology and some domains are even tens of micrometers in size. However, from $x = 0.005$, the domain area began to decrease and for higher concentrations, there are no domains with micrometer in size existing. It seems that the decrease of domain area starts after a critical concentration around $x = 0.005$. In ref 28, there is indeed a critical concentration (n_{0c}), which is determined by the ratio V_{cpl}/σ, as $2^{1/2}\pi^{-1/2}(V_{cpl}/\sigma)n_{0c}^{1/2} = 1$. In our system, V_{cpl} can be estimated by the interaction energy between GM1 and DOPC-rich L_d phase, or the energy of breaking the van der Waals interaction between DOPC molecules due to the insertion of GM1, which is 0.4−4 kJ/mol,[29] and σ is related to the line tension (γ) between SM/Chol and DOPC by $\gamma = \sigma h$, where h is the membrane thickness. Taking $h \sim 5$ nm, and $\gamma = 1.2$ pN,[30] the critical impurity density n_{0c} is estimated to be around 0.006, which is consistent with our experimental observation. When $x < 0.005$, GM1 concentration is extremely low in DOPC-rich L_d phase, and the whole interaction energy between these GM1 molecules with DOPC phase is too low to compete with the interfacial tension between the L_o and L_d phases. Therefore the unfavorable interaction between GM1 and DOPC can be neglected in the free energy of the system. This conclusion explains why at $x = 0.001$, there is no eminent change in morphology. The concentration $x = 0.005$ is close to this critical concentration, exhibiting the potential pinning effect in Figure 2c. As the GM1 concentration increases in mixtures, to reduce the unfavorable interaction between GM1 and DOPC, DOPC tends to form domains at the place where local GM1 concentration is low. This dynamic process is reflected by the observation of small amount of GM1 in L_d phases. As the GM1 concentration continuously increases, the unfavorable interaction of GM1 and DOPC becomes dominant and controls the final domain size, and the domain growth is pinned at sufficient high GM1 concentrations.

3.3. In Situ GM1 Insertion. By assuming the less mobile GM1 as impurities in SM/DOPC/Chol membranes, we connected the morphology change with the underlying domain dynamics. Meanwhile, domain growth may be affected by temperature, incubation time,[17] cooling rate,[31] and so on. Would a similar change happen if we gradually insert the GM1 molecules into SM/DOPC/Chol bilayer with time?

Recent researches have proved that GM1 molecules can automatically insert into membranes from its water solution.[13,32] The insertion is a slow process and the GM1 concentration in bilayer gradually increases with time. Inspired by this fact, we designed in situ GM1 insertion experiment into a well-formed SM/DOPC/Chol (=2:2:1) bilayer to further investigate the morphology change with increasing GM1 concentration. The experimental conditions were carefully controlled as described in Section 2.6. If we assume that the GM1 molecules injected into the fluid cell all inserted into the upper membrane, when GM1 water solution was $\sim 5 \times 10^{-6}$ mg/mL, the total amount of GM1 injected once into the fluid cell was ~0.001 (in mole fraction) of the lipid mixtures on the mica. For the GM1 water solution with high GM1 concentration used, the amount of GM1 injected was ~0.005. However, we note that GM1 molecules in water solutions could not all insert into membrane in a short period,

dx.doi.org/10.1021/jp2008122 |J. Phys. Chem. B 2011, 115, 5923–5929

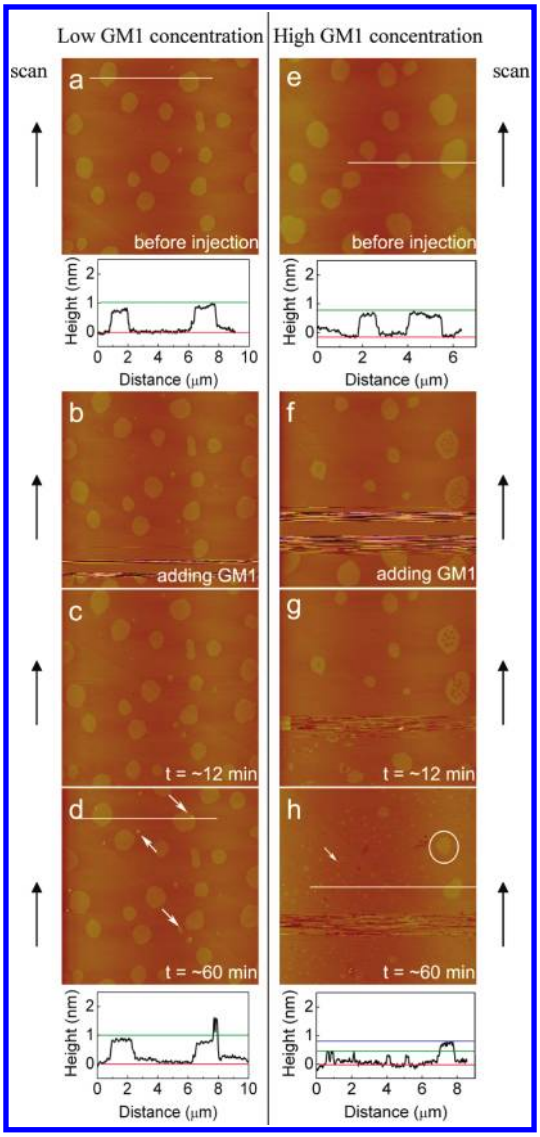

Figure 6. in situ GM1 insertions within 60 min. The GM1 concentrations of these GM1 water solutions are 5×10^{-6} mg/mL (low GM1 concentration, a−d) and 2.4×10^{-5} mg/mL (higher GM1 concentration, e−h), respectively. The size for a−d is 14 μm × 14 μm and for e−h is10 μm × 10 μm. Before GM1 insertion, the mole ratio of SM/DOPC/Chol for each composition is 2:2:1.

which can be proven by Bach et al., who detected that only ~30% of GM1 molecules can truly transfer from water into the membranes.[32] Therefore the above estimation is the upper limit that the amount of GM1 molecules could enter into the membranes. We are not able to measure the exact amount of GM1 that finally inserted into bilayers here, but this does not change our qualitative analyses below.

The images in Figure 6a−d show that, by incubating the bilayer with GM1 water solution of a low concentration, the GM1 molecules inserted into the bilayer and formed small dots/aggregations in both SM-rich domain and DOPC-rich domains, as observed in Figure 6d. These dots mainly locate at the edges of the SM-rich L_o domains, and some locate in DOPC-rich L_d phases. The increased height is 0.6−0.9 nm, which is consistent with our previous observation and the literature data.[24] These GM1 dots can insert into the membrane because the lipid packing at the edges of the L_o and L_d domains, as well as in the L_d phases, is relatively loose. Clearly, when GM1 concentration is quite low, the GM1 molecules do not strongly affect the well-formed lateral phase-separated structures.

However, when the bilayer was incubated with water solution of the high GM1 concentration (Figures 6e−h), the initial micrometer-scale SM-rich domains (with height ~1 nm) were destroyed and broken down, and nanometer-scale new L_o domains (with height 0.4−0.9 nm) reassembled and emerged in the bilayer. These phenomena indicated that with the increasing GM1 concentration in the bilayer, large SM-rich domain cannot retain and the size of L_o domain cannot grow into micrometer scale. At the late stage of the insertion, the domain growth was pinned by the relative high GM1 concentration. Moreover, referring to Figure 2, one can related the small dots in Figure 6h (with height ~0.5 nm, as the arrow pointed) with those we observed at high GM1 concentrations, indicating the new L_o domains are GM1-rich; and those larger domains (with height ~0.9 nm, as circled) are similar to those observed at low and intermediate GM1 concentrations in section 3.2, which are SM-rich or GM1/SM mixtures.

Therefore, the experiments of inserting GM1 molecules into bilayers further support our conclusion that with sufficiently high GM1 concentration, the domain growth in lateral phase separation of SM/DOPC/Chol bilayers is indeed pinned by the presence of the GM1 molecules.

4. CONCLUSION

We studied how GM1 concentrations affect the lateral phase separation in SM/DOPC/cholesterol supported lipid bilayers using AFM in aqueous environment. We observed that increasing GM1 mol fraction (x) leads to the change in the dominant component of the liquid-ordered phase (L_o domains), from SM to SM/GM1 mixtures and finally to GM1. Meanwhile, the area of the L_o domains (A) decreases with the increase of GM1 concentration, following a scaling law as $A \sim x^{-3/2}$ for $x > 0.005$. This trend agrees with the conclusion of previous computer simulation on the phase separation in binary fluid containing fixed impurities, indicating that the domain growth here is pinned by high concentration of GM1 molecules. Such concentration effect of GM1 on phase separation is further supported by the in situ GM1 insertion experiments.

The structure of GSLs varies greatly in both acyl chains lengths and headgroup compositions.[6,7] Rather than numerous investigations of each GSL molecule, general rules are needed to understand how these molecules influence the lateral phase separations of the membranes. Here, by simplifying one representative GSL molecule as impurities, we connected morphology change with domain growth and provided a more general way to estimate the distribution of GSLs and their influence on phase separation. Moreover, these results intrigued us to further investigate on the dynamics of lateral phase separation with GSLs in lipid mixtures.

AUTHOR INFORMATION

Corresponding Author

*E-mail: fengqiu@fudan.edu.cn. Telephone: 0086-21-5566-4036. Fax: 0086-21-6564-0293.

■ ACKNOWLEDGMENT

We gratefully acknowledge the financial support from The National High Technology Research and Development Program of China (Grant No. 2008AA032101) and Natural Science Foundation of China (Grant No. 20874021).

■ REFERENCES

(1) Simons, K.; Ikonen, E. *Nature* **1997**, *387*, 569.
(2) Simons, K.; Toomre, D. *Nat. Rev. Mol. Cell Biol.* **2000**, *1*, 31.
(3) Binder, W. H.; Barragan, V.; Menger, F. M. *Angew. Chem., Int. Ed.* **2003**, *42*, 5802.
(4) Dietrich, C.; Bagatolli, L. A.; Volovyk, Z. N.; Thompson, N. L.; Levi, M.; Jacobson, K.; Gratton., E. *Biophys. J.* **2001**, *80*, 1417.
(5) Veatch, S. L.; Keller, S. L. *Phys. Rev. Lett.* **2005**, *94*, 148101.
(6) Cantu, L.; Corti, M.; Brocca, P.; Favero, E. D. *Biochim. Biophys. Acta, Biomembr.* **2009**, *1788*, 202.
(7) Prinetti, A.; Loberto, N.; Chigorno, V.; Sonnino, S. *Biochim. Biophys. Acta, Biomembr.* **2009**, *1788*, 184.
(8) Fishman, P. H. *J. Membr. Biol.* **1982**, *69*, 85.
(9) Thomas, P. D.; Brewer, G. J. *Biochim. Biophys. Acta* **1990**, *1031*, 277.
(10) Vié, V.; Van Mau, N.; Lesniewska, E.; Goudonnet, J. P.; Heitz, F.; Le Grimellec, C. *Langmuir* **1998**, *14*, 4574.
(11) Yokoyama, S.; Ohta, Y.; Sakai, H.; Abe, M. *Colloids Surf., B* **2004**, *34*, 65.
(12) Ohta, Y.; Yokoyama, S.; Sakai, H.; Abe, M. *Colloids Surf., B* **2004**, *34*, 147.
(13) Reich, C.; Horton, M. R.; Krause, B.; Gast, A. P.; Rädler, J. O.; Nickel, B. *Biophys. J.* **2008**, *95*, 657.
(14) Yuan, C.; Furlong, J.; Burgos, P.; Johnston, L. J. *Biophys. J.* **2002**, *82*, 2526.
(15) Yuan, C.; Johnston, L. J. *Biophys. J.* **2001**, *81*, 1059.
(16) Ferraretto, A.; Pitto, M.; Palestini, P.; Masserini, M. *Biochemistry* **1997**, *36*, 9232.
(17) Mao, Y.; Shang, Z; Imai, Y.; Hoshino, T.; Tero, R.; Tanaka, K.; Yamamoto, N.; Yanagisawa, K.; Urisu, T. *Biochim. Biophys. Acta, Biomembr.* **2010**, *1798*, 1090.
(18) Coban, O.; Burger, M.; Laliberte, M.; Ianoul, A.; Johnston, L. J. *Langmuir* **2007**, *23*, 6704.
(19) Connell, S. D.; Smith, D. A. *Mol. Membr. Biol.* **2006**, *23*, 17.
(20) Richter, R. P.; Bérat, R.; Brisson, A. R. *Langmuir* **2006**, *22*, 3497.
(21) Basu, A.; Glew, R. H. *J. Biol. Chem.* **1985**, *260*, 13067.
(22) Patel, R. Y.; Balaji, P. V. *J. Phys. Chem. B* **2008**, *112*, 3346.
(23) Tashima, Y.; Oe, R.; Lee, S.; Sugihara, G.; Chambers, E. J.; Takahashi, M.; Yamada, T. *J. Biol. Chem.* **2004**, *279*, 17587.
(24) Lawrence, J. C.; Saslowsky, D. E.; Edwardson, J. M.; Henderson, R. M. *Biophys. J.* **2003**, *84*, 1827.
(25) Wang, R.; Shi, J.; Parikh, A. N.; Shreve, A. P.; Chen, L.; Swanson, B. I. *Colloids Surf., B* **2004**, *33*, 45.
(26) Mondal, S.; Mukhopadhyay, C. *Langmuir* **2008**, *24*, 10298.
(27) Goins, B.; Masserini, M.; Barisas, B. G.; Freire, E. *Biophys. J.* **1986**, *49*, 849.
(28) Qiu, F.; Peng, G.; Ginzburg, V. V.; Balazs, A. C.; Chen, H.-Y.; Jasnow, D. *J. Chem. Phys.* **2001**, *115*, 3779.
(29) Garrett, R.; Grisham, C. M. *Biochemistry*, 4th ed.; Cengage Learning: Stamford, 2009; Chapter 1.
(30) García-Sáez, A. J.; Chiantia, S.; Schwille, P. *J. Biol. Chem.* **2007**, *282*, 33537.
(31) Goksu, E. I.; Vanegas, J. M.; Blanchette, C. D.; Lin, W.; Longo, M. L. *Biochim. Biophys. Acta, Biomembr.* **2009**, *1788*, 254.
(32) Bach, D.; Miller, I. R.; Sela, B.-A. *Biochim. Biophys. Acta* **1982**, *686*, 233.